Mild and Cost-Effective One-Pot Synthesis of Pure Single-Crystalline β-Ag$_{0.33}$V$_2$O$_5$ Nanowires for Rechargeable Li-ion Batteries

Wen Hu, Xin-bo Zhang,* Yong-liang Cheng, Chao-yong Wu, Feng Cao, and Li-min Wang*[a]

Much attention has been given to reversible electricity storage in rechargeable batteries due to the potential applications in electric vehicles and renewable energy systems based on intermittent sources (e.g., wind and solar power). Among all advanced battery systems, lithium-ion batteries (LIBs) have taken less than 20 years to successfully capture the portable electronics market. However, great improvements in storage capacity are required to conquer the upcoming electric transportation and renewable energy markets. Storage capacity is currently mainly limited by the electrode materials, especially at the cathode side.[1] Solutions require new concepts in order to to break through the one-electron redox chemistry limitation (i.e., 1 e$^-$ per 3d metal) of classical lithium insertion/deinsertion reactions.[2] Combination displacement/intercalation (CDI) electrode reactions,[3] which enable multielectron charge transfers, can lead to impressive capacity gains and thus greatly expand the range of cathode choices. This is due to the ability of both sites occupied by transition metals and vacant sites within the host structure to provide sites for Li$^+$ ions, while traditional intercalation pathways are only able to utilize sites that are already vacant.[4] Unfortunately, the initial crystal structure of the electrode material is not fully recovered after repeated CDI processes (due to decomposition and recrystallization), which in theory prohibits a long cycle life.[5] Therefore, the development of new concepts to effectively retain the crystal structure of high-capacity cathode materials upon continuous CDI processes is very important.

Metal vanadates are one of the most important families of functional inorganic materials, and owing to their layered nature they have found numerous applications in the fields of catalysis,[6] optical devices,[7] magnetic materials,[8] and battery materials.[4a, 9] Silver vanadium oxide (Ag$_2$V$_4$O$_{11}$; SVO) has been used commercially as high-capacity cathode material, based on the CDI mechanism, in medical primary LIBs.[4, 9a, 10] Unfortunately, the crystal structure of SVO can not be retrieved after repeated CDI processes due to incompatibility between the radii of Ag$^+$ (1.15 Å, employed to sustain the (V$_4$O$_{11}$)$_n$ layered structure in SVO) and Li$^+$ (0.76 Å), and the large valence difference between V^{5+} and V^{3+}, which theoretically impedes the application of Ag$_2$V$_4$O$_{11}$ in rechargeable lithium ion batteries.[4b, 11]

To improve the retrievability of the crystal structure, we turn to nonstoichiometric SVO: Ag$_{1-x}$V$_2$O$_5$, $0 < x < 1$. When the silver content is decreased, a more rigid three-dimensional (V$_2$O$_5$)$_n$ tunnel framework, in which VO$_5$ pyramids "glue" each (V$_4$O$_{11}$)$_n$ layer, can be constructed. Hence, the preservation of the crystal structure no longer depends solely on interlayer Ag$^+$ and, once successfully synthesized, the Ag$^+$/Li$^+$ displacement reaction has less influence on the host framework. In addition, Ag$^+$ doping would partially lower the valence state of V^{5+} (because of charge balance), which alleviates the valence change of vanadium during Li$^+$ insertion. Both could facilitate the recrystallization of the initial structure and improve the reversibility of the CDI process. Although several methods have been developed to prepare nonstoichiometric SVO (e.g., pulsed laser deposition, sputtering, classical solid-state synthesis, the V$_2$O$_5$ aerogel template method, and the surfactant-assisted hydrothermal approach),[12] all suffer from (more or less severe) drawbacks such as the necessity of using special equipment or costly low-valence vanadium precursors (e.g., V$_2$O$_4$ or V$_2$O$_3$), complicated preparation processes, energy- and/or time-consuming procedures, inability of large-scale fabrication, and especially product impurity, which is inherent to the agent employed to reduce V^{5+} simultaneously reducing Ag$^+$ to Ag^0, contaminating Ag$_{1-x}$V$_2$O$_5$ with Ag^0 particles. In addition, it is recognized that nanowire-based materials in LIBs can offer the potential for significant improvements in power and energy density over bulk electrodes, due to their very large surface-to-volume ratio to contact the electrolyte, continuous conducting pathways for electrons through the electrodes, facile strain relaxation during battery operation, and other advantages.[13] Up to now, neither the simple fabrication of pure nonstoichiometric SVO nor the synthesis of 1D nanowires (NWs) of this material have been reported. Thus, to explore new strategies to effectively synthesize pure Ag$_{1-x}$V$_2$O$_5$ NWs in a time- and cost-effective manner, and exploring its electrochemical performance, is highly desirable.

Herein, we present a facile, mild, and efficient method for the one-pot synthesis of pure β-Ag$_{0.33}$V$_2$O$_5$ (β-SVO) NWs, in which acetophenone, serving as reducing agent, plays a decisive role. Electrochemical measurements show that the obtained compound has a high discharge capacity (up to 239 mAh g^{-1}). Most importantly, the β-SVO crystal phase is maintained even after eight consecutive discharge/charge cycles, clearly demonstrating that our proposed strategy to improve the structure retrievability during the CDI process is very effective. Furthermore, the data presented here can provide helpful information for the operating mechanisms and cycle life of lithium intercalation into transition metal vanadates based on the CDI mechanism.

[a] Dr. W. Hu, Prof. Dr. X.-b. Zhang, Dr. Y.-l. Cheng, Dr. C.-y. Wu, Dr. F. Cao, Dr. L.-m. Wang
State Key Laboratory of Rare Earth Resource Utilization
Changchun Institute of Applied Chemistry, Chinese Academy of Sciences
Changchun 130022 (PR China)
Fax: (+86) 431-85262447
E-mail: xbzhang@ciac.jl.cn
lmwang@ciac.jl.cn

AgNO$_3$ and V$_2$O$_5$ were used as metal ion sources, and acetophenone was employed as reducing agent in a hydrothermal redox polymerization process for the preparation of the β-SVO NWs. Neither templates nor surfactants were used, and importantly all of the reagents used in the present reaction system are very cheap. Although acetophenone has previously been used as ligand and/or stabilizer agent,[14] we are the first to exploit its reducibility and effectively synthesize β-SVO NWs. Figure 1 shows the reaction process and formation mechanism of the β-SVO NWs. Large amounts of benzoic acid were found in the final reaction solution (Figure S1). The oxidation of acetophenone to benzoic acid might account for the formation of the V^{4+} and V^{3+} in the β-SVO product from the V^{5+} precursors, in which the appropriate reducing strength of acetophenone plays a key role to ensure the high purity of the product. The obtained β-SVO nuclei aggregated and grew into lamellar microstructures according to the well-known Ostwald ripening mechanism.[4a, 9a] As the reaction proceeded the internal tension induced a "splitting" process to lower the total energy, during which the layered β-SVO gradually split into β-SVO nanosheets and finally split into NWs.

X-ray diffraction (XRD) patterns (Figure 2a) show Bragg peaks that are consistent with a monoclinic β-Ag$_{0.33}$V$_2$O$_5$ phase (space group C2/m, JCPDS file number 01-081-1740). Interestingly, no reflections that can be ascribed to Ag^0, a contaminant that generally exists in β-SVO prepared by other methods as described above, are detected, indicating the high purity of the β-SVO material prepared here. High-resolution photoelectron spectroscopy (XPS; Figure S3) reveals that the silver species in the β-SVO sample is only Ag$^+$ with no signal of Ag^0, and that a small fraction of the V^{5+} is reduced to V^{4+} and even V^{3+}. This is in good agreement with the XRD results. Energy dispersive X-ray spectroscopy (EDS; Figure S4) shows that the as-synthesized NWs are composed of Ag, V, and O and that the atomic ratio of Ag to V is 0.172, which is close to the nominal value. All of the these results indicate the successful synthesis of pure β-Ag$_{0.33}$V$_2$O$_5$.
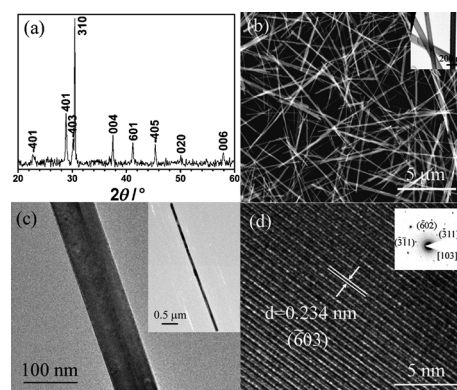

Figure 2. a) XRD, b) SEM, c) TEM, and d) HRTEM images of the as-synthesized β-Ag$_{0.33}$V$_2$O$_5$ nanowires. The inset in (b) is a magnified SEM image, that in (c) is an overview image of a single nanowire, and that in (d) is the [103] SAED pattern.

Typical SEM (Figure 2b) and TEM (Figure 2c) images show the morphology of the as-synthesized β-Ag$_{0.33}$V$_2$O$_5$ material: a well-defined 1D material tens of micrometers long and with a uniform diameter of ca. 70 nm. The microstructure of the product was further studied by high-resolution transmission electron microscopy (HRTEM) and selected-area electron diffraction (SAED). Figure 2d shows a HRTEM image of a single crystal that reveals the (603) lattice planes of β-Ag$_{0.33}$V$_2$O$_5$. In addition, SAED patterns were measured along two different zone axes. One measurement was taken along the [103] zone axis (Figure 2d, inset), deduced from an analysis of the distances and angles of the array of discrete diffraction spots, while the other taken along the [010] zone axis is unconventional but interesting. A detailed analysis of the [010] SAED pattern is shown in Figure S5. Both SAED patterns confirmed the single-crystalline nature of the β-SVO. In conclusion, the as-synthesized product comprises highly pure, single-crystalline β-Ag$_{0.33}$V$_2$O$_5$ nanowires (see Figure S6 for a crystal structure), as confirmed by XRD, XPS, EDS, SAED, and HRTEM results.

The cathode performance of the β-Ag$_{0.33}$V$_2$O$_5$ NWs was tested with respect to lithium metal. A typical galvanostatic signature in the voltage window of 2–3.6 V at 20 mA g^{-1} is shown in Figure 3a. Notably, the discharge capacity at the third cycle is 239 mAh g^{-1} (1.95 Li$^+$ uptake), similar to that of the first cycle. This is because the β-SVO crystal structure is fully recovered once the electrode is recharged to 3.4 V, as evidenced by the ex situ XRD pattern (Figure 4a) and Ag 3d XPS spectrum (Figure S7a), showing the return of Ag$^+$ as an indication of metallic silver oxidation followed by reinjection into the β-
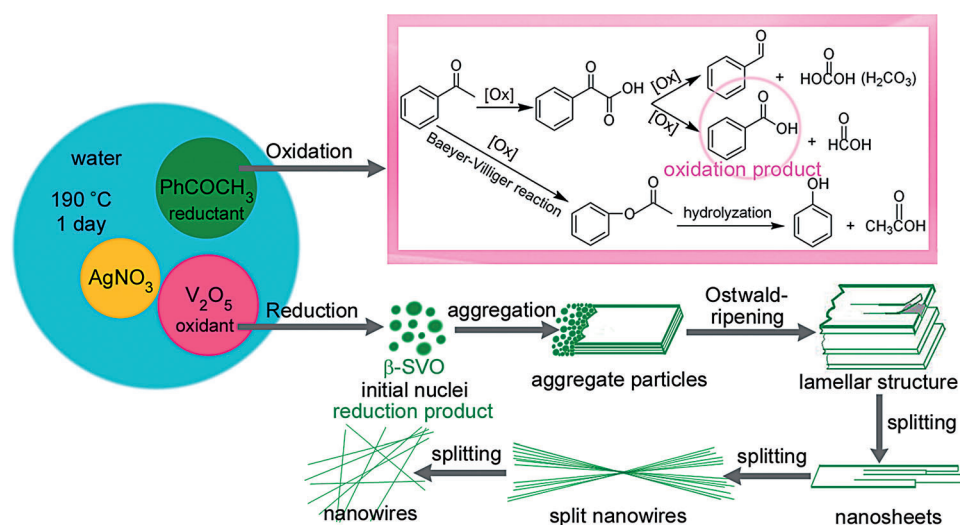

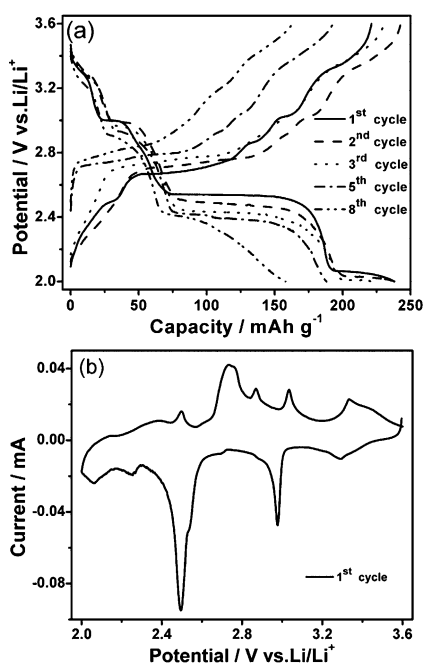**Figure 1.** Illustration of the chemical reaction mechanisms and morphological evolution in the synthesis of β-Ag$_{0.33}$V$_2$O$_5$ nanowires.

Figure 3. a) Discharge–charge profiles of the β-Ag$_{0.33}$V$_2$O$_5$ electrode at 20 mAg^{-1} in the voltage range of 2–3.6 V. b) CV curve in the first cycle at a scan rate of 0.01 mV s^{-1} in the voltage range of 2–3.6 V.
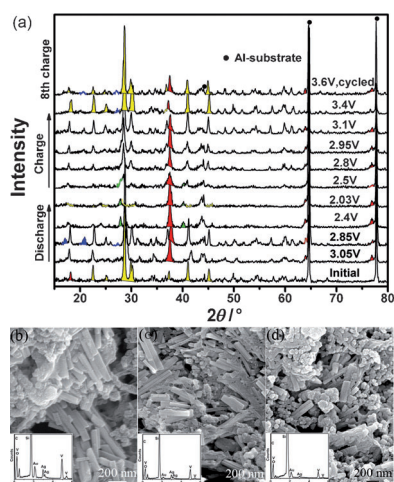

Figure 4. a) Ex situ XRD patterns of β-Ag$_{0.33}$V$_2$O$_5$ electrode, as fabricated, discharged or charged to different voltage depths and charged to 3.6 V after 8 cycles. The yellow Bragg peaks refer to the β-Ag$_{0.33}$V$_2$O$_5$ phase, indicative of its crystalline structure preservation even after eight cycles testing. The red Bragg peaks refer to metallic Ag. The blue Bragg peaks refer to the formation of the inert ε-LiV$_2$O$_5$ phase, and the green Bragg peaks refer to the intermediate γ-Li$_2$V$_2$O$_5$ phase. The other panels show SEM images and EDS patterns of b) bare electrode, c) electrode recharged to 3.4 V, and d) charged electrode to 3.6 V after 8 cycles.

SVO framework. This is in contrast to the closely related material Ag$_2$V$_4$O$_{11}$ where the reinjection of silver does not induce recrystallization into the original structure. Furthermore, multiple voltage plateaus due to different redox reactions associated with lithium insertion/extraction can be observed in the charge and discharge curves, which presents a striking contrast to the inclined profile of other SVO cathodes.[4b, 9a, 15] These

redox reactions can be better illustrated by using cyclic voltammetry (CV) curves (Figure S8). In combination with the ex situ XRD patterns of β-SVO electrodes recovered from multiple cells discharged or charged to selected voltage (Figure 4a), the three main reduction peaks located at 3.29, 2.98, and 2.50 V for the first discharge (Figure 3b) can be reasonably assigned to successive phase transformations upon lithium ion insertion into β-Ag$_{0.33}$V$_2$O$_5$, giving metallic Ag^0, ε-LiV$_2$O$_5$, and γ-Li$_2$V$_2$O$_5$, respectively. Specifically, when the discharge progresses to 3.05 V, all the silver in the β-SVO is released as Ag$^+$, but only Ag^0 is detected by XPS (Figure S7b), indicating the discharge rate of Ag$^+$ to Ag^0 is faster than the reduction of V^{5+}. Notably, even after eight cycles of discharge and charge, the crystal structure of the initial β-SVO can still be recovered (Figure 4a). This good retrievability highlights the feasibility and strength of our proposed concept for improving the reversibility of decomposition and recrystallization of the initial electrode material during repeated CDI process. The discharge capacity deteriorates from the fifth cycle, which might be due to the pulverization of partial crystalline grains, as evidenced by the fracture and thus shortened NWs shown in Figure 4b–d despite the preservation of the 1D NW morphology. NWs with larger surface-to-volume ratios might possess better strain relaxation properties—relevant research work is in progress.

In summary, we report a facile, mild, cost-effective, one-pot method for the large-scale synthesis of pure β-Ag$_{0.33}$V$_2$O$_5$ nanowires. Neither template nor surfactant is used, while the appropriate reducing strength of acetophenone plays a decisive role. When tested as cathode material, the β-Ag$_{0.33}$V$_2$O$_5$ nanowires show a reversible uptake of 1.95 Li$^+$ ions per formula. Furthermore, the crystal structure of the nanowires reamins unchanged, even after several cycles. These results provide useful information on lithium intercalation into transition metal vanadates based on the combination displacement/intercalation mechanism. The successful realization of our proposed strategy in the case of β-Ag$_{0.33}$V$_2$O$_5$ can be extended to other systems, so as to develop higher-capacity cathodes for high-capacity lithium-ion batteries.

Experimental Section

Chemicals and materials: We used silver nitrate (AgNO$_3$, Beijing Chemical Works, AR), vanadium pentoxide (V$_2$O$_5$, Beijing Chemical Works, AR), acetophenone (C$_8$H$_8$O, Sinopharm Chemical Reagent Co., Ltd., AR), dichloromethane (CH$_2$Cl$_2$, Beijing Chemical Works, AR), deionized water, Absolute alcohol, acetylene black (Hong-xin Chemical Works), polyvinylidenefluoride (PVDF, DuPont company, 99.9%), N-methyl-2-pyrrolidinone (NMP, Aladdin Reagent, AR), separator (polypropylene film, Celgard), and electrolyte (1 M LiPF$_6$ in ethylene carbonate/dimethyl carbonate (EC/DMC) at a weight ratio of 1:1, Zhangjiagang Guotai-Huarong New Chemical Materials Co., Ltd). All chemicals were used as-received.

Synthesis: Stoichiometric amounts of AgNO$_3$ (0.0163 g) and V$_2$O$_5$ (0.0436 g) were dispersed in 24 mL deionized water blended with 50 μL acetophenone. After the mixture had been stirred and after ultrasonication for 10 min, the mixture was transferred into a 30 mL Teflon-linked stainless steel autoclave and maintained at 190 °C for 1 day, then allowed to cool to room temperature. A

greenish–black gel-like solid was obtained, which overflowed all of the inner lining. The solid was collected by centrifugation, washed with deionized water and ethanol, and then dried under vacuum at 70 °C for 12 h.

Characterization: To investigate the phase structure of the obtained products, XRD patterns were recorded by a Bruker D8 Focus power X-ray diffractometer with Cu Kα radiation. SEM was performed by a Hitachi S-4800 field emission scanning electron microscopy instrument, whereas EDS was carried out by using a Bruker AXS microanalysis instrument at an accelerating voltage of 20 kV. A Philips TF-F20 (200 kV) transmission electron microscope with an energy-dispersive X-ray spectrometer was used to obtain SAED patterns and local compositional information and to study the phase microstructure. The oxidation states of the constituent elements were measured by XPS using Thermo ESCALAB 250 system and the XPSPEAK software was used for the fitting of the XPS spectra. GC–MS analysis was carried out by using an Agilent 6890N-5975 device. The final aqueous reaction solution after removal of the solid precipitates was extracted with anhydrous dichloromethane three times, and then injected into the GC device. Electrochemical measurement: The positive electrodes were fabricated by mixing 80 wt% active materials, 10 wt% acetylene black, and 10 wt% PVDF binder in an appropriate amount of NMP as solvent. The resulting paste was then spread on an aluminum foil by an automatic film coater with vacuum pump & micrometer doctor blade (MTI). After the NMP solvent evaporation in a vacuum oven at 120 °C for 12 h, the electrodes were pressed and cut into disks. A CR2032 coin-type cell was assembled with lithium metal as the counter and reference electrode and polypropylene film as a separator. The cells were constructed and handled in an argon-filled glovebox. The charge–discharge measurements were carried out using the Land battery system (CT2001A) at a constant current density in a voltage range of 2–3.6 V versus Li/Li$^+$. The cyclic voltammetric measurements were performed using a VMP3 electrochemical workstation (Bio-logic Inc.). The cells, discharged/charged to different voltages and maintained at that voltage for 3 h, were opened in the glovebox, and the positive electrodes were washed with DMC and dried in a vacuum oven at 90 °C for 12 h. Then the working electrodes were analyzed by XRD and XPS, and the materials scratched off the electrodes were analyzed by SEM–EDX.

Acknowledgements

[1] a) M. Winter, R. J. Brodd, *Chem. Rev.* **2004**, *104*, 4245–4269; b) M. S. Whittingham, *Chem. Rev.* **2004**, *104*, 4271–4301; c) P. G. Bruce, B. Scrosati, J.-M. Tarascon, *Angew. Chem.* **2008**, *120*, 2972–2989; *Angew. Chem. Int. Ed.* **2008**, *47*, 2930–2946; d) J. M. Tarascon, M. Armand, *Nature* **2001**, *414*, 359–367; e) A. S. Aricò, P. Bruce, B. Scrosati, J.-M. Tarascon, W. van Schalkwijk, *Nat. Mater.* **2005**, *4*, 366–377.

[2] a) A. K. Padhi, K. S. Nanjundaswamy, J. B. Goodenough, *J. Electrochem. Soc.* **1997**, *144*, 1188–1194; b) S.-Y. Chung, J. T. Bloking, Y.- M. Chiang, *Nat. Mater.* **2002**, *1*, 123–128; c) K. Mizushima, P. C. Jones, P. J. Wiseman, J. B. Goodenough, *Solid State Ionics* **1981**, *3–4*, 171–174; d) Y. Nishi, *Chem. Rec.* **2001**, *1*, 406–413.

[3] a) M. Morcrette, P. Rozier, L. Dupont, E. Mugnier, L. Sannier, J. Galy, J.-M. Tarascon, *Nat. Mater.* **2003**, *2*, 755–761; b) M. Morcrette, P. Martin, P. Rozier, H. Vezin, F. Chevallier, L. Laffont, P. Poizot, J.-M. Tarascon, *Chem. Mater.* **2005**, *17*, 418–426; c) V. Bodenez, L. Dupont, M. Morcrette, C. Surcin, D. W. Murphy, J.-M. Tarascon, *Chem. Mater.* **2006**, *18*, 4278–4287.

[4] a) H. Ma, S. Y. Zhang, W. Q. Ji, Z. L. Tao, J. Chen, *J. Am. Chem. Soc.* **2008**, *130*, 5361–5367; b) F. Sauvage, V. Bodenez, J.-M. Tarascon, K. R. Poeppelmeier, *J. Am. Chem. Soc.* **2010**, *132*, 6778–6782.

[5] J. B. Goodenough, Y. Kim, *Chem. Mater.* **2010**, *22*, 587–603.

[6] a) Y. Zhao, Y. Xie, S. Yan, S. X. Wang, *Chem. Eur. J.* **2008**, *14*, 1601–1606; b) A. Kudo, K. Omori, H. Kato, *J. Am. Chem. Soc.* **1999**, *121*, 11459–11467.

[7] a) B. Peng, Z. C. Fan, X. M. Qiu, L. Jiang, G. H. Tang, H. D. Ford, W. Huang, *Adv. Mater.* **2005**, *17*, 857–859; b) A. Huignard, T. Gacoin, J.-P. Boilot, *Chem. Mater.* **2000**, *12*, 1090–1094; c) J. W. Stouwdam, M. Raudsepp, F. C. J. M. van Veggel, *Langmuir* **2005**, *21*, 7003–7008.

[8] Z. Z. He, J.-I. Yamaura, Y. Ueda, W. D. Cheng, *J. Am. Chem. Soc.* **2009**, *131*, 7554–7555.

[9] a) S. Y. Zhang, W. Y. Li, C. S. Li, J. Chen, *J. Phys. Chem. B* **2006**, *110*, 24855–24863; b) Y. T. Kim Gopukumar, K. B. Kim, B. W. Cho, *J. Power Sources* **2002**, *112*, 504–508; c) S.-H. Ng, N. Tran, K. G. Bramnik, H. Hibst, P. Novak, *Chem. Eur. J.* **2008**, *14*, 11141–11148; d) L. F. Xiao, Y. Q. Zhao, J. Yin, L. Z. Zhang, *Chem. Eur. J.* **2009**, *15*, 9442–9450; e) J. M. Song, Y. Z. Lin, H. B. Yao, F. J. Fan, X. G. Li, S. H. Yu, *ACS Nano* **2009**, *3*, 653–660; f) L. Zhou, W. J. Cui, J. M. Wu, Q. F. Zhao, H. X. Li, Y. Y. Xia, Y. H. Wang, C. Z. Yu, *Nanoscale* **2011**, *3*, 999–1003.

[10] a) E. S. Takeuchi, W. C. Thiebolt III, *J. Electrochem. Soc.* **1988**, *135*, 2691–2694; < lit b>T. A. Albrecht, F. Sauvage, V. Bodenez, J.-M. Tarascon, K. R. Poeppelmeier, *Chem. Mater.* **2009**, *21*, 3017–3020.

[11] a) F. Sauvage, V. Bodenez, H. Vezin, M. Morcrette, J.-M. Tarascon, K. R. Poeppelmeier, *J. Power Sources* **2010**, *195*, 1195–1201; b) F. Sauvage, V. Bodenez, H. Vezin, T. A. Albrecht, J.-M. Tarascon, K. R. Poeppelmeier, *Inorg. Chem.* **2008**, *47*, 8464–8472.

[12] a) Y. Q. Chu, Q. Z. Qin, *Chem. Mater.* **2002**, *14*, 3152–3157; b) W. Gulbinski, T. Suszko, W. Sienicki, B. Warcholinski, *Wear* **2003**, *254*, 129–135; c) E. Déramond, J. M. Savarialt, J. Galy, *Acta Crystallogr. Sect. C* **1994**, *50*, 164–166; d) F. Coustier, J. Hill, B. B. Owens, S. Passerini, W. H. Smyrl, *J. Electrochem. Soc.* **1999**, *146*, 1355–1360; e) C. R. Xiong, A. E. Aliev, B. Gnade, K. J. Balkus, *ACS Nano* **2008**, *2*, 293–301.

[13] a) C. K. Chan, X. F. Zhang, Y. Cui, *Nano Lett.* **2007**, *7*, 307–309; b) C. K. Chan, H. L. Peng, G. Liu, K. McIlwrath, X. F. Zhang, R. A. Huggins, Y. Cui, *Nat. Nanotechnol.* **2008**, *3*, 31–35.

[14] a) M. Niederberger, G. Garnweitner, *Chem. Eur. J.* **2006**, *12*, 7282–7302; b) M. Niederberger, G. Garnweitner, *Mater. Res. Soc. Symp. Proc.* **2005**, *879E*, Z9.8.1- Z9.8.5.

[15] Z. J. Chen, S. K. Gao, R. H. Li, M. D. Wei, K. M. Wei, H. S. Zhou, *Electrochim. Acta* **2008**, *53*, 8134–8137.